J Fluoresc (2016) 26:835–844
DOI 10.1007/s10895-016-1771-x

ORIGINAL ARTICLE

A Turn-on Fluorescent Chemosensor for Zn^{2+} Based on Quinoline in Aqueous Media

Yong Sung Kim[1] · Jae Jun Lee[1] · Sun Young Lee[1] · Pan-Gi Kim[2] · Cheal Kim[1]

Received: 19 November 2015 / Accepted: 14 January 2016 / Published online: 21 January 2016

Abstract A simple "off-on fluorescence type" chemosensor **1** 3-((2-(dimethylamino)ethyl)amino)-N-(quinolin-8-yl)propanamide has been synthesized for Zn^{2+}. The receptor **1** comprises the quinoline moiety as fluorophore and the N,N′-dimethylethane-1,2-diamine as a binding site. **1** showed a remarkable fluorescence enhancement in the presence of Zn^{2+} in aqueous solution. Importantly, the chemosensor **1** could be used to detect and quantify Zn^{2+} in water samples. In particular, this chemosensor could clearly distinguish Zn^{2+} from Cd^{2+}. The binding properties of **1** with Zn^{2+} ions were investigated by UV-vis, fluorescence, electrospray ionization mass spectroscopy and ^{1}H NMR titration.

Keywords Fluorescence enhancement · Determination of Zn ion · Chemosensor · Quinoline

Introduction

Zinc is the second most abundant transition metal ion in human body [1–7]. Zinc has attracted a great deal of attention [8–13], because it plays very important role in variety of physiological and pathological processes such as apoptosis, catalytic function of protein, enzyme regulation and so on [14–20]. Especially, labile Zn^{2+} has been implicated in signaling processes in the brain, immunological function and gene transcription [21–24]. Its deficiency generates unbalanced metabolism, which in turn can induce retarded growth in children, brain disorders and high blood cholesterol, and also be implicated in various neurodegenerative disorders such as Alzheimer's disease, epilepsy, ischemic stroke, and infantile diarrhea. Excess zinc may also cause serious neurological disorders such as Alzheimer's and Parkinson's diseases [25–28]. Thus, a technique to detect and visualize free zinc ions would be highly demanded [29–34].

To date, many chemosensors have been reported to detect trace amount of Zn^{2+}. Many of them, however, have disadvantages such as insufficient sensitivity or selectivity, and inhibition problems from other transition metal ions, especially Cd^{2+}, which is in the same group of the periodic table and shows similar properties to Zn^{2+} [35–38]. Thus, low cost and easily prepared Zn^{2+} selective fluorescence chemosensors are needed for convenience [39–45].

In view of this necessity and as part of our effort devoted to zinc ion recognition, we have considered the combination of a quinoline moiety known as having desirable photo-physical properties as a fluorophore group and a N, N′-dimethyl ethylene amine as a binding site (Scheme 1) [46–48]. Especially, we expected that the N, N′-dimethyl ethylene amine group, being hydrophilic in nature, would increase water-solubility of the chemosensor.

Herein, we report a new chemosensor **1** for Zn^{2+}, composed of the quinoline and N, N′-dimethyl ethylene amine moieties. We have observed its prominent fluorescence enhancement in the presence of zinc ion, while there was no enhancement in the presence of other metal ions. In particular, it was able to distinguish Zn^{2+} from Cd^{2+}.

Electronic supplementary material The online version of this article (doi:10.1007/s10895-016-1771-x) contains supplementary material, which is available to authorized users.

✉ Cheal Kim
chealkim@snut.ac.kr

[1] Department of Fine Chemistry and Department of Interdisciplinary Bio IT Materials, Seoul National University of Science and Technology, Seoul 139-743, Republic of Korea

[2] School of Ecology & Environmental Systems, Kyungpook National University, Sangju 37224, South Korea

Scheme 1 Synthetic procedure of **1**

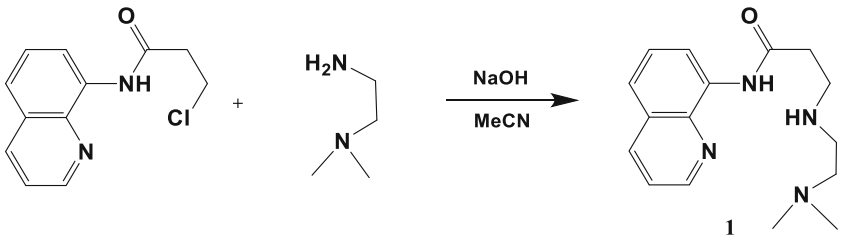

Experiments

Reagents and Instrument

All the solvents and reagents (analytical grade and spectroscopic grade) were obtained commercially and used as received. ^{1}H and ^{13}C NMR spectra were recorded on a Varian 400 MHz and 100 MHz spectrometer, respectively and chemical shifts were reported in ppm, relative to tetramethylsilane $Si(CH_3)_4$. Absorption spectra were recorded at 25 °C using a Perkin Elmer model Lambda 25 UV/Vis spectrometer. The emission spectra were recorded on a Perkin-Elmer LS45 fluorescence spectrometer. Electrospray ionization mass spectra (ESI-MS) were collected on a Thermo Finnigan (San Jose, CA, USA) LCQTM Advantage MAX quadrupole ion trap instrument. Elemental analysis for carbon, nitrogen, and hydrogen was carried out by using a Flash EA 1112 elemental analyzer (thermo) in Organic Chemistry Research Center of Sogang University, Korea.

Synthesis of Receptor 1

3-Chloro-N-(quinolin-8-yl)propanamide (1.17 g, 5 mmol) and potassium iodide (8 mmol, 1.33 g) were dissolved in MeCN (20 mL) and stirred for 1 h. Then, N,N′-dimethylethane-1,2-diamine (0.44 mL, 5 mmol) and sodium hydroxide (0.24 g, 6 mmol) were added in the resulting solution. It was stirred for 12 h at room temperature. The solvent was removed under reduced pressure to obtain bright yellow oil, which was dissolved in methylene chloride and washed twice with water. Then, the solution was purified by silica gel column chromatography (10:1 *v*/v CH_2Cl_2-CH_3OH) (Scheme 1). The solvent was evaporated under vacuo. Yield: 0.97 g (68 %). ^{1}H NMR (400 MHz, DMSO-d_6, ppm): δ = 10.59 (s, 1 H), 8.85 (d, *J* = 4 Hz, 1 H), 8.51 (d, *J* = 8 Hz, 1 H), 8.27 (d, *J* = 8 Hz, 1 H), 7.52 (d, *J* = 4 Hz, 1 H), 7.50 (t, *J* = 4 Hz, 1 H), 7.38 (t, *J* = 8 Hz, 1 H), 2.97 (t, *J* = 6.4 Hz, 4 H), 2.79 (t, *J* = 6.4 Hz, 4 H), 2.41 (s, 6 H); ^{13}C NMR (100 MHz, CD_3CN, ppm): 163.09, 162.82, 162.52, 149.15, 137.13, 136.03, 127.05, 122.31, 122.12, 116.65, 55.77, 49.11, 48.73, 43.54, 35.09, 27.59. LRMS (ESI): m/z calcd for $C_{16}H_{22}N_4O$-H^++Zn^{2+}: 547.23; found 547.20. Elemental analysis calcd (%) for $C_{16}H_{23}N_4$: C, 67.11; H, 7.74; N, 19.56; found: C, 66.87; H, 7.92; N, 19.83.

Fluorescence Titration of 1 Toward Zn^{2+}

The receptor **1** (1.72 mg, 0.006 mmol) was dissolved in MeCN (2 mL) and 20 μL of the receptor **1** (3 mM) was diluted to 2.98 mL MeCN/bis-tris buffer solution (3:7, *v*/v) to make the final concentration of 20 μM. $Zn(NO_3)_2$ $6H_2O$ (11.9 mg, 0.04 mmol) was dissolved in MeCN (2 mL) and 3–36 μL of the Zn^{2+} solution (20 mM) was transferred to each receptor

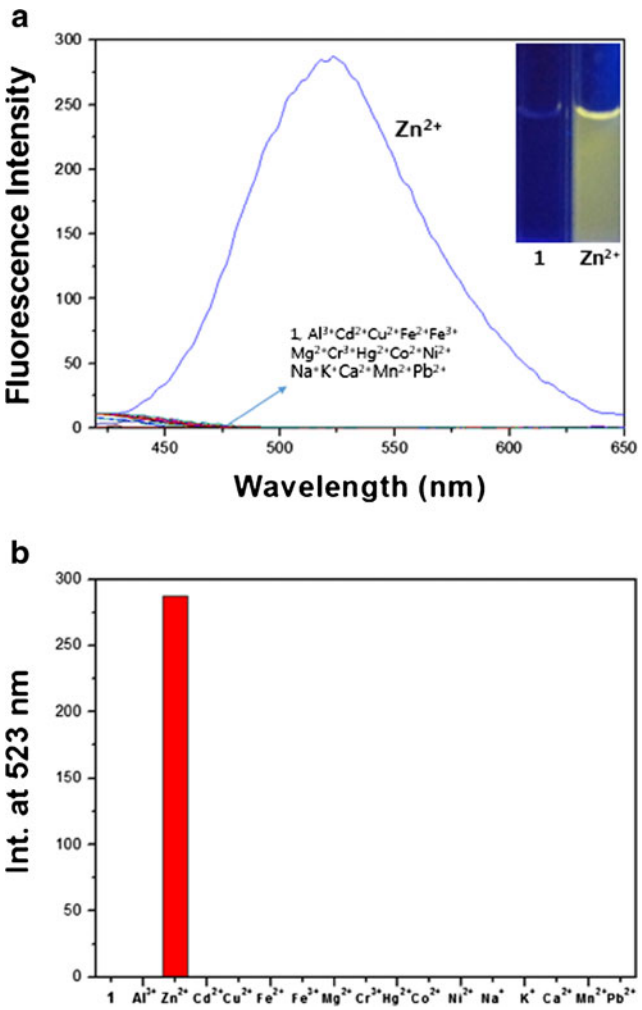

Fig. 1 Fluorescence spectral changes of **1** (20 μM) in the presence of different metal ions (12 equiv) such as Al^{3+}, Zn^{2+}, Cd^{2+}, Cu^{2+}, Fe^{2+}, Fe^{3+}, Mg^{2+}, Cr^{3+}, Hg^{2+}, Co^{2+}, Ni^{2+}, Na^{+}, K^{+}, Ca^{2+}, Mn^{2+} and Pb^{2+} with an excitation of 523 nm in a mixture of MeCN/bis-tris buffer solution (3:7, *v*/v)

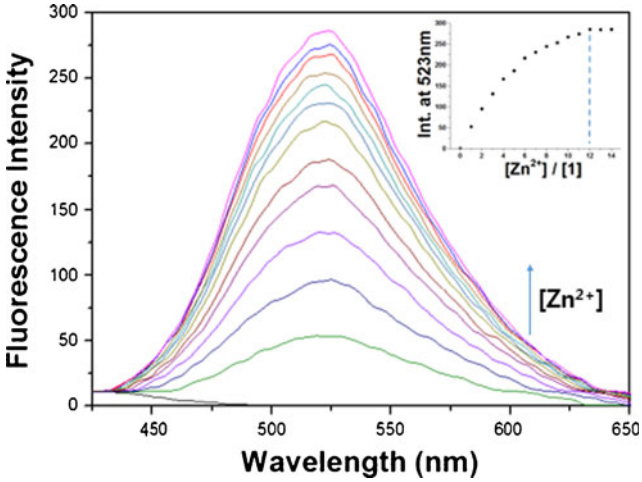

Fig. 2 Fluorescence spectral changes of **1** (20 μM) in the presence of different concentrations of Zn^{2+} ions in a mixture of MeCN/bis-tris buffer solution (3:7, *v*/v). Inset: Fluorescence intensity at 523 nm versus the number of equiv. of Zn^{2+} added

solutions prepared above. After mixing them for a few seconds, fluorescence spectra were taken at room temperature.

UV-vis Titration of 1 Toward Zn^{2+}

The receptor **1** (1.72 mg, 0.006 mmol) was dissolved in MeCN (2 mL) and 30 μL of the receptor **1** (3 mM) were diluted to 2.97 mL MeCN/bis-tris buffer solution (3:7, *v*/v) to make the final concentration of 30 μM. $Zn(NO_3)_2\ 6H_2O$ (11.9 mg, 0.04 mmol) was dissolved in MeCN (2 mL) and 0.9–9 μL of the Zn^{2+} solution (20 mM) were added to the receptor **1** solution prepared above. After mixing them for a few seconds, UV-vis spectra were obtained at room temperature.

Job Plot Measurements

The receptor **1** (1.72 mg, 0.006 mmol) was dissolved in MeCN (2 mL). 500 μL of the receptor solution was taken and diluted with MeCN/bis-tris buffer solution (3:7, *v*/v) to make the final concentration of 50 μM. The total volume of the receptor solution was 30 mL. $Zn(NO_3)_2\ 6H_2O$ (11.9 mg, 0.04 mmol) was dissolved in MeCN (2 mL). 75 μL of the zinc solution was taken and diluted with MeCN/bis-tris buffer solution (3:7, *v*/v). The total volume of zinc solution was 30 mL. 0.3, 0.6, 0.9, 1.2, 1.5, 1.8, 2.1, 2.4 and 2.7 mL of the **1** solution were taken and transferred to vials. 2.7, 2.4, 2.1, 1.8, 1.5, 1.2, 0.9, 0.6 and 0.3 mL of the zinc solution were added to each diluted **1** solution. Each vial had a total volume of 3 mL. After reacting them for a few seconds, fluorescence spectra were taken at room temperature.

Competition with Other Metal Ions

The receptor **1** (1.72 mg, 0.006 mmol) was dissolved in MeCN (2 mL) and 20 μL of this solution (3 mM) was diluted with 2.98 mL of MeCN/bis-tris buffer solution (3:7, *v*/v) to make the final concentration of 20 μM. MNO_3 (M = Na, K, 0.04 mmol) or $M(NO_3)_2$ (M = Zn, Cd, Cu, Mg, Co, Ni, Ca, Mn and Pb, 0.04 mmol) or $M(NO_3)_3$ (M = Al, Fe and Cr, 0.04 mmol) or $M(ClO_4)_2$ (M = Fe, 0.04 mmol) was separately dissolved in MeCN (2 mL). 36 μL of Zn^{2+} solution and each metal solution were taken, respectively, and added to receptor **1** prepared above to give 12 equiv. After mixing them for a few seconds, fluorescence spectra were obtained at room temperature.

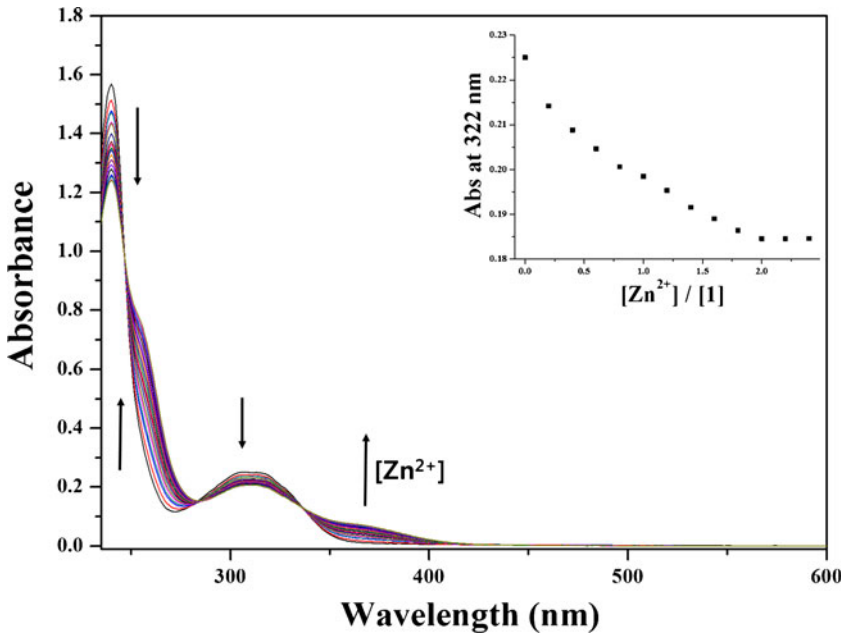

Fig. 3 UV-vis titration of **1** (30 μM) with Zn^{2+} (0–2 equiv). Inset: Absorption titration profile of **1** with Zn^{2+} at 322 nm

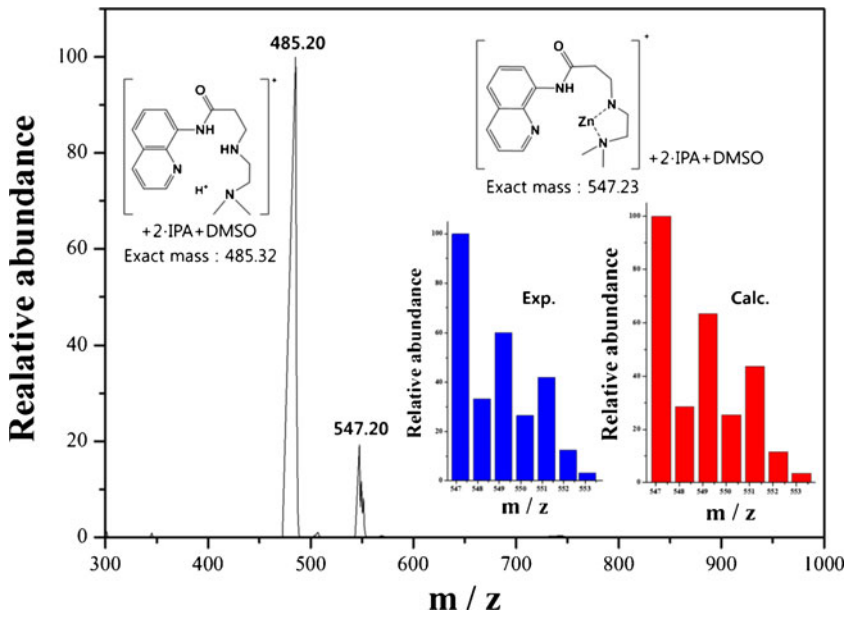

Fig. 4 Positive-ion electrospray ionization mass spectrum of **1** (100 μM) upon addition of $Zn(NO_3)_2$ (1 equiv)

pH Effect Test of 1 Toward Zn^{2+}

A series of buffers with pH values ranging from 2 to 12 was prepared by mixing sodium hydroxide solution and hydrochloric acid in bis-tris buffer. After the solution with a desired pH was achieved, receptor **1** (1.72 mg, 0.006 mmol) was dissolved in MeCN (2 mL), and then 20 μL of the receptor **1** (3 mM) were diluted with 2.98 mL MeCN/bis-tris buffer solution (3:7, *v*/v) to make the final concentration of 20 μM. $Zn(NO_3)_2\ 6H_2O$ (11.9 mg, 0.04 mmol) was dissolved in MeCN (2 mL). 36 μL of the Zn2+ solution (20 mM) were transferred to each receptor solution (20 μM) prepared above. After mixing them for a few seconds, fluorescence spectra were obtained at room temperature.

NMR Titration of 1 Toward Zn^{2+}

Four NMR tubes of **1** (0.28 mg, 0.01 mmol) dissolved in CD_3CN (0.7 mL) were prepared, and four different equiv. (0, 0.5, 0.8 and 1 equiv) of zinc nitrate dissolved in CD_3CN (0.3 mL) were added separately to the solutions of **1**. After shaking them for a few seconds, the ^1H NMR spectra were taken.

Determination of Zn^{2+} in Water Samples

Fluorescence spectral measurements of water samples containing Zn^{2+} were performed by adding 20 μL of 3 mmol/L stock solution of **1** and 0.60 mL of 50 mmol/L bis-tris buffer

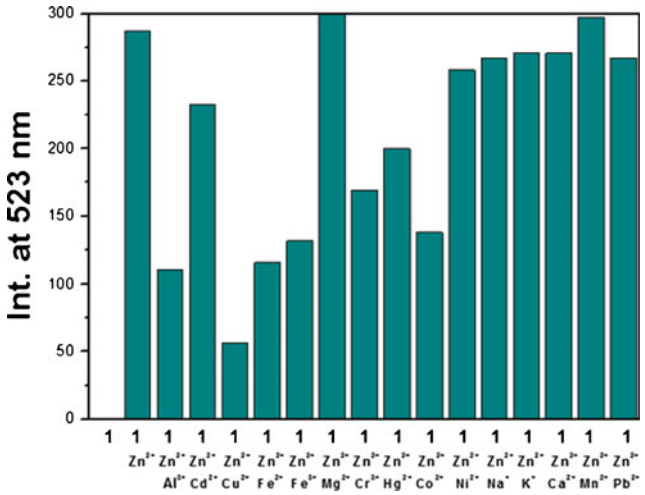

Fig. 5 Competitive selectivity of **1** (20 μM) toward Zn^{2+} (12 equiv) in the presence of other metal ions (12 equiv) with an excitation of 370 nm in a mixture of MeCN/bis-tris buffer solution (3:7, *v*/v)

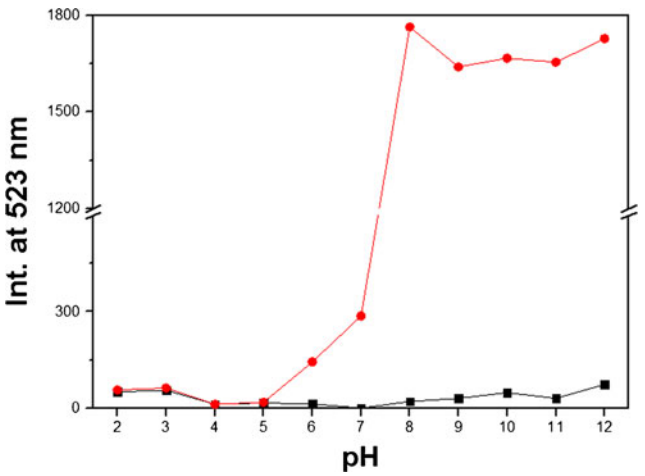

Fig. 6 Fluorescence intensity (at 523 nm) of **1** (20 μM) in the presence of Zn^{2+} at different pH values (2–12) in a mixture of MeCN/bis-tris buffer solution (3:7, *v*/v)

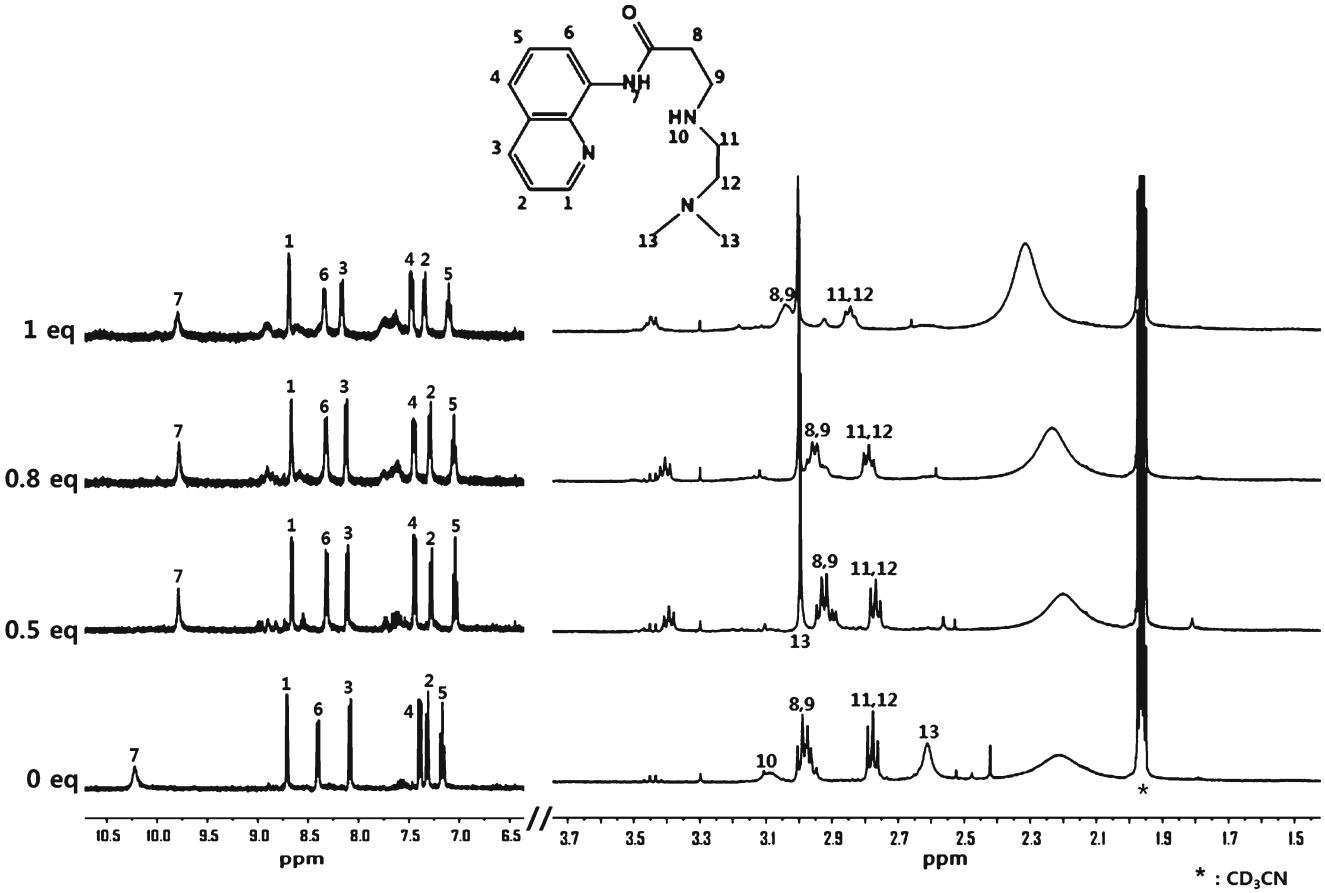

Fig. 7 ^{1}H NMR titration of **1** with $Zn(NO_3)_2$ $6H_2O$

solution to 2.38 mL sample solutions. After well mixed, the solutions were allowed to stand at 25 °C for 2 min before the test.

Theoretical Calculation Methods

All DFT/TDDFT calculations based on the hybrid exchange-correlation functional B3LYP [49, 50] were carried out using Gaussian 03 program [51]. The 6-31G** basis set [52, 53] was used for the main group elements, whereas the Lanl2DZ effective core potential (ECP) [54, 55] was employed for Zn. In vibrational frequency calculations, there was no imaginary frequency for the optimized geometries of **1** and **1**-Zn^{2+}, suggesting that these geometries represented local minima. For all calculations, the solvent effect of water was considered by using the Cossi and Barone's CPCM (conductor-like polarizable continuum model) [56, 57]. To investigate the electronic properties of singlet excited states, time-dependent DFT (TDDFT) was performed in the ground state geometries of **1** and **1**-Zn^{2+}. Thirty lowest singlet states were calculated and analyzed. The GaussSum 2.1 [58] was used to calculate the contributions of molecular orbital in electronic transitions.

Scheme 2 Fluorescence enhancement mechanism and proposed structure of **1**-Zn^{2+} complex

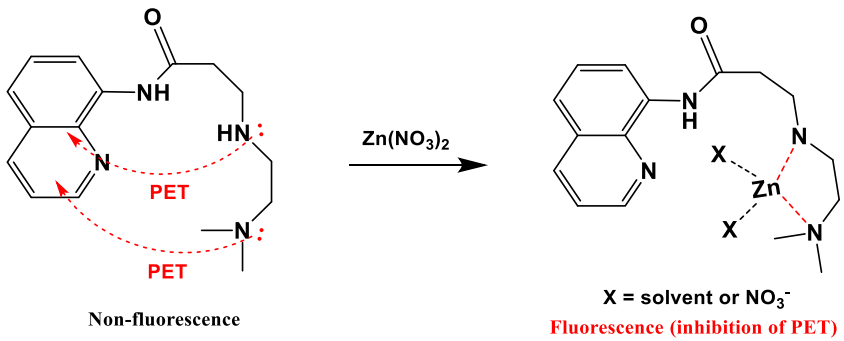

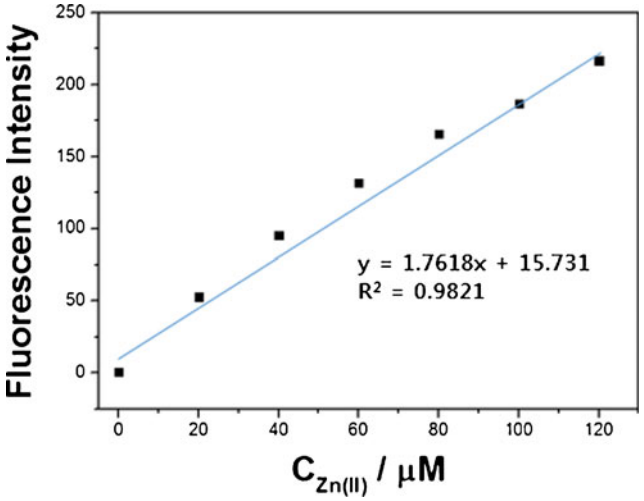

Fig. 8 Fluorescence intensity (at 523 nm) of **1** as a function of Zn(II) concentration. [**1**] = 20 μmol/L, [Zn(II)] = 0–120 μmol/L. Conditions: all samples were conducted in a mixture of MeCN/bis-tris buffer solution (3:7, *v*/v). λ_{ex} and λ_{em} were 370 and 523 nm, respectively

Results and Discussion

Synthesis of 1

The compound **1** 3-((2-(dimethylamino)ethyl)amino)-N-(quinolin-8-yl)propanamide was synthesized by substitution reaction of 3-chloro-N-(quinolin-8-yl)propanamide and N,N′-dimethyl ethylene amine in acetonitrile (Scheme 1), and characterized by ^{1}H NMR, ^{13}C NMR, elemental analysis and ESI-mass spectrometry.

Fluorescence and Absorption Spectroscopic Studies of 1 Toward Zn^{2+}

The fluorometric behavior of the receptor **1** toward various metal ions was studied in a mixture of MeCN/bis-tris buffer solution (3:7, *v*/v). When excited at 370 nm, receptor **1** exhibited a weak fluorescence emission (λ_{max} = 523 nm) compared to that (424 folds) in the presence of Zn^{2+} (Fig. 1). By contrast, upon addition of other metal ions such as Al^{3+}, Cd^{2+}, Cu^{2+}, Fe^{2+}, Fe^{3+}, Mg^{2+}, Cr^{3+}, Hg^{2+}, Co^{2+}, Ni^{2+}, Na^{+}, K^{+}, Ca^{2+}, Mn^{2+} and Pb^{2+}, either no or slight increase in intensity was observed. These results indicated that the receptor **1** could be used as a fluorescence chemosensor for Zn^{2+} and discriminate Zn^{2+} from Cd^{2+} [59–63]. Moreover, we examined the fluorometric properties of **1** with Zn^{2+} in polar and non-polar solvents such as chloroform, methanol (MeOH), acetonitrile (MeCN) and N,N-dimethylformamide (DMF) (Fig. S1). **1** displayed strong fluorescence with Zn^{2+}, which featured a red-shift with increase of the solvent polarity.

Table 1 Determination of Zn(II) in water samples

Sample	Zn(II) added (μmol/L)	Zn(II) found (μmol/L)	Recovery (%)	R.S.D. (*n* = 3) (%)
Tap water	0.00	0.00		
	4.00	4.12	103.0	0.37
Water sample	0.00	0.00		
	4.00 [a]	9.82	98.2	1.88

[a] Synthesized by deionized water, 6.00 μmol/L Zn(II), 10 μmol/L Cd(II), Pb(II), Na(I), K(I), Ca(II), Mg(II). Conditions: [**1**] = 20 μmol/L in 10 mM MeCN:bis-tris buffer solution (3:7, pH 7.0)

To further investigate the chemosensing properties of **1**, fluorescence titration of the receptor **1** with Zn^{2+} ion was carried out. As shown in Fig. 2, the emission intensity of **1** at 523 nm gradually increased until the amount of Zn^{2+} reached 12 equiv. The binding properties of **1** with Zn^{2+} were further studied by UV-vis titration experiments (Fig. 3). UV-vis absorption spectrum of **1** showed two absorption bands at 240 nm and 310 nm. Upon the addition of Zn^{2+} ion to the solution of **1**, the two bands have red-shifted to 257 and 367 nm, respectively. Meanwhile, three clear isosbestic points were observed at 246 nm, 283 and 336 nm, implying the undoubted conversion of free **1** to a zinc complex.

The Job plot showed a 1:1 complexation stoichiometry between **1** and Zn^{2+} (Fig. S2) [64], which was further confirmed by ESI-mass spectrometry analysis (Fig. 4). The positive-ion mass spectrum of **1** upon addition of 1 equiv. of Zn^{2+} showed the formation of the [**1**-H^{+}+Zn^{2+}+2IPA+DMSO]$^{+}$ [m/z: 547.20; calcd, 547.23]. From the fluorescence titration data, the association constant for **1** with Zn^{2+} was determined as 1.4 x 10^{4} M^{-1} using Benesi-Hildebrand method (Fig. S3) [65]. This value is within the range of those (1.0 ~ 1.0 x 10^{12}) reported for Zn^{2+} sensing chemosensors [66–68]. The limit of detection was estimated to check the efficiency of the probe, which was based on the 3σ/slope (Fig. S4) [69, 70]. The detection limit for Zn^{2+} was determined as 7.1 μM, which was much lower than the WHO guideline (76 μM) for Zn^{2+} ions in drinking water [71, 72].

To explore the ability of **1** as a fluorescence receptor for Zn^{2+}, interference experiments were performed in the presence of Zn^{2+} (12 equiv) mixed with various metal ions (12 equiv) (Fig. 5). There was no interruption for the detection of Zn^{2+} in the presence of Mg^{2+}, Hg^{2+}, Ni^{2+}, Na^{+}, K^{+}, Ca^{2+}, Mn^{2+} and Pb^{2+}, while relatively low detectable responses were observed in the presence of Al^{3+}, Cu^{2+}, Fe^{2+}, Fe^{3+}, Cr^{3+} and Co^{2+}. On the other hand, Cd^{2+} ion hardly inhibited the fluorescence intensity of **1**-Zn^{2+}. These results suggest that **1** could be a good sensor for Zn^{2+} and, indeed, distinguish Zn^{2+} from Cd^{2+} commonly having similar properties in the same group of the periodic table.

The pH dependence of the **1**-Zn^{2+} complex was examined. Over the pH range tested, the fluorescence

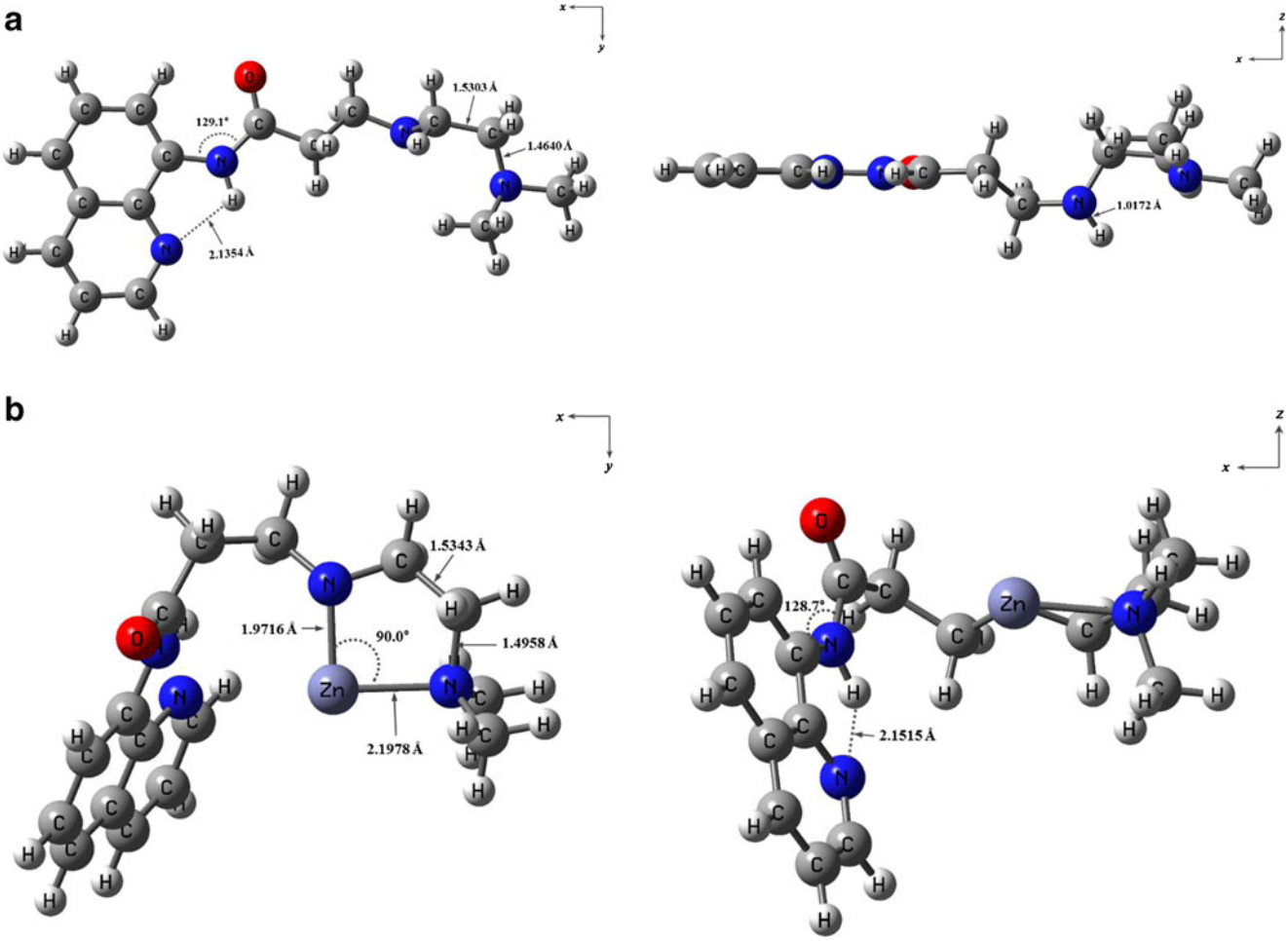

Fig. 9 Energy minimized structures of (a) **1** and (b) **1**-Zn^{2+}

intensity of **1**-Zn^{2+} displayed strong pH dependence (Fig. 6). An intense and stable fluorescence of **1**-Zn^{2+} found in the pH range of 7.0–12.0 warrants its application under physiological conditions, without any change in detection results.

^{1}H NMR Spectroscopic Studies of 1 Toward Zn^{2+}

The ^{1}H NMR titration experiments were studied to further examine the binding mode between **1** and Zn^{2+} ion (Fig. 7). Upon addition of Zn^{2+} to receptor **1**, H_{10} disappeared at 0.5 equiv. H_8, H_9, H_{11}, H_{12} and H_{13} showed significantly downfield shift, while H_7 shifted upfield and the protons in quinoline slightly shifted downfield or upfield. There was no shift in the position of proton signals on further addition of Zn^{2+} (>1.0 equiv). These results suggest that two nitrogen atoms in dimethyl ethylene amine might coordinate to Zn^{2+} ion (Scheme 2). Based on these results, we proposed that the low fluorescence of **1** could be due to photoinduced electron transfer (PET) from lone-pair electrons of receptor (dimethyl ethylene amine) to fluorophore (quinolone). Thus, 'off-on' fluorescence of **1** caused by Zn^{2+} might be attributed to the inhibition of PET (Scheme 2).

Determination of Zinc ion in Water Samples

We constructed a calibration curve for the determination of Zn^{2+} by **1** (Fig. 8). Receptor **1** showed a good linear relationship between the fluorescence intensity of **1** and Zn^{2+} concentration (0–120 μM) with a correlation coefficient of R^2 = 0.9821 (n = 3). This result indicates that **1** is suitable for quantitative detection of Zn^{2+}. In order to examine the applicability of the receptor **1** in environmental samples, the chemosensor was applied for the determination of Zn^{2+} in water samples. First, tap water samples were chosen. As shown in Table 1, one can see a satisfactory recovery and R.S.D. values of water samples. Also, we prepared artificial polluted water samples by adding various metal ions known as being involved in industrial processes into deionized water. The results were also summarized in Table 1, which exhibited a satisfactory recovery and R.S.D. values for the artificial water samples.

Theoretical Calculations

To gain an insight into fluorescent sensing mechanism for **1**-Zn^{2+}, time-dependent density functional theory (TD-DFT) calculations were performed at the optimized geometries (S_0) of **1** and **1**-Zn^{2+} complex (Fig. 9). In case of **1**, the main molecular orbital (MO) contributions of the first lowest excited states were determined for HOMO → LUMO and HOMO - 1 → LUMO transition (332.82 nm, Fig. S5). As shown in Fig. S6, HOMO - 1 → LUMO of **1** indicates π → π* transition in quinoline moiety, which means radiative transition. HOMO → LUMO of **1** indicates PET from dimethyl ethylene amine to quionline, which could explain the non-radiative process of **1**. For **1**-Zn^{2+} complex (Fig. S7), the third lowest excited state was considered as main transition of **1**-Zn^{2+} complex (oscillator strength = 0.1317), while its first lowest excited state showed minor transition (oscillator strength = 0.0284). The main molecular orbital (MO) contribution of the third lowest excited state was determined for HOMO - 1 → LUMO (330.48 nm). As shown in Fig. S5, it shows π → π* transition in quinoline moiety, which indicates radiative transition. Thus, these results suggested that the sensing mechanism of **1** toward Zn^{2+} was originated by inhibition of PET process [73].

Conclusion

We have synthesized a new fluorescent chemosensor **1**, which displays high sensitivity and selectivity toward zinc in aqueous media. The complexation of **1** with Zn^{2+} exhibited a pronounced enhancement in the fluorescence emission. Moreover, the detection limit (7.1 μM) is much lower than the WHO detection level (76 μM) for Zn^{2+} ions in drinking water. Most importantly, recovery studies of the water samples added with Zn^{2+} demonstrated its value in the practical application. Therefore, we believe that receptor **1** will be a prototype for the practicable system for detecting Zn^{2+} concentrations in environmental systems.

Acknowledgments Financial support from Basic Science Research Program through the National Research Foundation of Korea (NRF) funded by the Ministry of Education, Science and Technology (NRF-2014R1A2A1A11051794 and NRF-2015R1A2A2A09001301) are gratefully acknowledged.

References

1. Upadhyay KK, Kumar A (2010) Pyrimidine based highly sensitive fluorescent receptor for Al^{3+} showing dual signalling mechanism. Org Biomol Chem 8:4892–4897
2. Karak D, Lohar S, Banerjee A, Sahana A, Hauli I, Mukhopadhyay SK, Matalobos JS, Das D (2012) Interaction of soft donor sites with a hard metal ion: crystallographically characterized blue emitting fluorescent probe for Al(III) with cell staining studies. RSC Adv 2: 12447–12454
3. Lee YJ, Seo D, Kwon JY, Son G, Park MS, Choi Y, Soh JH, Lee HN, Lee KD, Yoon J (2006) Anthracene derivatives bearing sulfur atoms or selenium atoms as fluorescent chemosensors for Cu^{2+} and Hg^{2+}: different selectivity induced from ligand immobilization onto anthracene. Tetrahedron 62:12340–12344
4. Kumar M, Kumar N, Bhalla V (2012) Ratiometric nanomolar detection of Cu^{2+} ion in mixed aqueous media: a Cu^{2+}/Li^{+} ions switchable allosteric system based on thia calix [4] crown. Dalton Trans 41:10189–10193
5. Kim KB, You DM, Jeon JH, Yeon YH, Kim JH, Kim C (2014) A fluorescent and colorimetric chemosensor for selective detection of aluminum in aqueous solution. Tetrahedron Lett 55:1347–1352
6. Tayade K, Sahoo SK, Chopra S, Singh N, Bondhopadhyay B, Basu A, Patil N, Attarde S, Kuwar A (2014) A fluorescent "turn-on" sensor for the biologically active Zn^{2+} ion. Inorg Chim Acta 421:538–543
7. Tayade K, Sahoo SK, Patil R, Singh N, Attarde S, Kuwar A (2014) 2, 2-[benzene-1, 2-diylbis(iminomethanediyl)]diphenol derivative bearing two amine and hydroxyl groups as fluorescent receptor for zinc (II) ion. Spectrochim Acta A 126:312–316
8. Liu Z, Zhang C, Chen Y, He W, Guo Z (2012) An excitation ratiometric Zn^{2+} sensor with mitochondria-target ability for monitoring of mitochondrial Zn^{2+} release upon different stimulations. Chem Commun 48:8365–8367
9. Choi YW, Park GJ, Na YJ, Jo HY, Lee SA, You GR, Kim C (2014) A single Schiff base molecule for recognizing multiple metal ions: a fluorescence sensor for Zn (II) and Al (III) and colorimetric sensor for Fe (II) and Fe (III). Sensors Actuators B Chem 194:343–352
10. Zhang C, Liu Z, Li Y, He W, Gao X, Guo Z (2013) In vitro and in vivo imaging application of a 1, 8-naphthalimide-derived Zn^{2+} fluorescent sensor with nuclear envelope penbility. Chem Commun 49: 11430–11432
11. Kim H, Kang J, Kim KB, Song EJ, Kim C (2014) A highly selective quinoline-based fluorescent sensor for Zn(II). Spectrochim Acta A 118:883–887
12. Guo Z, Kim G, Shin I, Yoon J (2012) A cyanine-based fluorescent sensor for detecting endogenous zinc ions in live cells and organisms. Biomaterials 33:7818–7827
13. Kim YS, Park GJ, Lee JJ, Lee SY, Kim C (2015) Multiple target chemosensor: a fluorescent sensor for Zn(II) and Al(III) and a chromogenic sensor for Fe(II) and Fe(III). RSC adv 5:11229–11239
14. O'Halloran TV (1993) Transition metals in control of gene expression. Science 261:715–725
15. Falchuk KH (1998) The molecular basis for the role of zinc in developmental biology. Mol Cell Biochem 188:41–48
16. Jiang PJ, Guo ZJ (2004) Fluorescent detection of zinc in biological systems: recent development on the design of chemosensors and biosensors. Coord Chem Rev 248:205–229
17. Maret W (2001) Zinc biochemistry, physiology, and homeostasis e recent insights and current trends. Biometals 14:187–190
18. Burdette SC, Lippard SJ (2003) Meeting of the minds: metalloneuro chemistry. Proc Natl Acad Sci U S A 100:3605–3610
19. Berg JM, Shi Y (1996) The galvanization of biology: a growing appreciation for the roles of zinc. Science 271:1081–1085
20. Vallee BL, Falchuk KH (1993) The biochemical basis of zinc physiology. Physiol Rev 73:79–118
21. Que EL, Domaille DW, Chang CJ (2008) Metals in neurobiology: probing their chemistry and biology with molecular imaging. Chem Rev 108:1517–1549
22. Dai Z, Canary JW (2007) Tailoring tripodal ligands for zinc sensing. New J Chem 31:1708–1718
23. Vallee BL, Auld DS (1993) Zinc: biological functions and coordination motifs. Acc Chem Res 26:543–551

24. Frederickson CJ, Suh SW, Silva D, Frederickson CJ, Thompson RB (2000) Maternal zinc supplementation during pregnancy affects autonomic function of Peruvian children assessed at 54 months of age. J Nutr 130:1471–1483
25. Bush AI, Pettingell WH, Paradis MD, Tanzi RE (1994) Modulation of a beta adhesiveness and secretase site cleavage by zinc. J Biol Chem 269:12152–12158
26. Cuajungco MP, Lees GJ (1997) Zinc metabolism in the brain: relevance to human neurodegenerative disorders. Neurobiol Dis 4: 137–169
27. Koh JY, Suh SW, Gwag BJ, He YY, Hsu CY, Choi DW (1996) Science 272:1013–1016
28. Kury S, Dreno B, Bezieau S, Giraudet S, Kharfi M, Kamoun R, Moisan JP (2002) Identification of *SLC39A4*, a gene involved in acrodermatitis enteropathica. Nat Genet 31:239–240
29. Zhu S, Zhang J, Janjanam J, Vegesna G, Luo FT, Tiwari A, Liu H (2013) Highly water-soluble BODIPY-based fluorescent probes for sensitive fluorescent sensing of zinc(II). J Mater Chem B 1:1722–1728
30. Ding Y, Xie Y, Li X, Hill JP, Zhang W, Zhu W (2011) Selective and sensitive "turn- on" fluorescent Zn^{2+} sensors based on di-and tripyrrins with readily modulated emission wavelengths. Chem Commun 47:5431–5433
31. Ding Y, Li T, Zhu W, Xie Y (2012) Highly selective colorimetric sensing of cyanide based on formation of dipyrrin adducts. Org Biomol Chem 10:4201–4207
32. Mei Y, Frederickson CJ, Giblin LJ, Weiss JH, Medvedeva Y, Bentley PA (2011) Sensitive and selective detection of zinc ions in neuronal vesicles using PYDPY1, a simple turn-on dipyrrin. Chem Commun 47:7107–7109
33. Yang Y, Zhao Q, Feng W, Li FY (2013) Luminescent chemodosimeters for bioimaging. Chem Rev 113:192–270
34. Qu L, Yin C, Huo F, Chao J, Zhang Y, Cheng F (2014) A pyridoxal-based dual chemosensor for visual detection of copper ion and ratiometric fluorescent detection of zinc ion. Sens Actuators B Chem 191:158–164
35. Nolan EM, Lippard SJ (2004) The zinspy family of fluorescent zinc sensors: syntheses and spectroscopic investigations. Inorg Chem 43:8310–8317
36. Aoki S, Kagata D, Shiro M, Takeda K, Kimura E (2004) Metal chelation-controlled twisted intramolecular charge transfer and its application to fluorescent sensing of metal ions and anions. J Am Chem Soc 126:13377–13390
37. Parkesh R, Lee TC, Gunnlaugsson T (2007) Highly selective 4-amino-1,8-naphthalimide based fluorescent photo induced electron transfer (PET) chemosensors for Zn(II) under physiological pH conditions. Org Biomol Chem 5:310–317
38. Park GJ, Lee MM, You GR, Choi YW, Kim C (2014) A turn-on and reversible fluorescence sensor with high affinity to Zn^{2+} in aqueous solution. Tetrahedron Lett 55:2517–2522
39. Lee YJ, Lim C, Suh H, Song EJ, Kim C (2014) A multifunctional sensor: chromogenic sensing for Mn^{2+} and fluorescent sensing for Zn^{2+} and Al^{3+}. Sensors Actuators B Chem 201:535–544
40. Song EJ, Park GJ, Lee JJ, Lee S, Noh I, Kim Y, Kim SJ, Kim C, Harrison RG (2015) A fluorescence sensor for Zn^{2+} that also acts as a visible sensor for Co^{2+} and Cu^{2+}. Sen. Actuators B 213:268–275
41. Kim H, You GR, Park GJ, Choi JY, Noh I, Kim Y, Kim SJ, Kim C, Harrison RG (2013) Selective zinc sensor based on pyrazoles and quinoline used to image cells. Dyes Pigments 113:723–729
42. Hanaoka K, Muramatsu Y, Urano Y, Terai T, Nagano T (2010) Design and synthesis of a highly sensitive off-on fluorescent chemosensor for zinc ions utilizing internal charge transfer. Chem Eur J 16:568–572
43. Xang D, Xiang X, Yang X, Wang X, Guo Y, Liu W, Qin W (2014) Fluorescein-based chromo-fluorescent probe for zinc in aqueous solution: spirolactam ring opened or closed? Sensors Actuators B Chem 201:246–254
44. Kim DH, Im YS, Kim H, Kim C (2014) Solvent-dependent selective fluorescence sensing of Al^{3+} and Zn^{2+}using a single Schiff base. Inorg Chem Commun 45:15–19
45. Zang L, Shang H, Wei D, Jiang S (2013) A multi-stimuli-responsive organogel based on salicylidene Schiff base. Sensors Actuators B Chem 185:389–397
46. Lee JJ, Lee SA, Kim H, Nguyen L, Noh I, Kim C (2015) A highly selective CHEF-type chemosensor for monitoring Zn^{2+} in aqueous solution and living cells. RSC Adv 5:41905–41913
47. Song EJ, Kang J, You GR, Park GJ, Kim Y, Kim SJ, Kim C, Harrison RG (2013) A single molecule that acts as a fluorescence sensor for zinc and cadmium and colorimetric sensor for cobalt. Dalton Trans 42:15514–15520
48. Kim JH, Hwang IH, Jang SP, Kang J, Kim S, Noh I, Kim Y, Kim C, Harrison RG (2013) Zinc sensors with lower binding affinities for cellular imaging. Dalton Trans 42:5500–5507
49. Becke AD (1993) Density-functional thermochemistry. III The role of exact exchange. J Chem Phys 98:5648–5652
50. Lee C, Yang W, Parr RG (1988) Development of the colle-salvetti correlation-energy formula into a functional of the electron density. Phys Rev B 37:785–789
51. Frisch MJ, Trucks GW, Schlegel HB, Scuseria GE, Robb MA, Cheeseman JR, Montgomery Jr JA, Vreven T, Kudin KN, Burant JC, Millam JM, Iyengar SS, Tomasi J, Barone V, Mennucci B, Cossi M, Scalmani G, Rega N, Petersson GA, Nakatsuji H, Hada M, Ehara M, Toyota K, Fukuda R, Hasegawa J, Ishida M, Nakajima T, Honda Y, Kitao O, Nakai H, Klene M, Li X, Knox JE, Hratchian HP, Cross JB, Bakken V, Adamo C, Jaramillo J, Gomperts R, Stratmann RE, Yazyev O, Austin AJ, Cammi R, Pomelli C, Ochterski JW, Ayala PY, Morokuma K, Voth GA, Salvador P, Dannenberg JJ, Zakrzewski VG, Dapprich S, Daniels AD, Strain MC, Farkas O, Malick DK, Rabuck AD, Raghavachari K, Foresman JB, Ortiz JV, Cui Q, Baboul AG, Clifford S, Cioslowski J, Stefanov BB, Liu G, Liashenko A, Piskorz P, Komaromi I, Martin RL, Fox DJ, Keith T, Al-Laham MA, Peng CY, Nanayakkara A, Challacombe M, Gill PMW, Johnson B, Chen W, Wong MW, Gonzalez C, and Pople JA, Gaussian 03, Revision D.01, Gaussian, Inc., Wallingford CT, 2004
52. Hariharan PC, Pople JA (1973) The influence of polarization functions on molecular orbital hydrogenation energies. Theor Chim Acta 28:213–222
53. Francl MM, Petro WJ, Hehre WJ, Binkley JS, Gordon MS, DeFrees DF, Pople JA (1982) Self-consitent molecular orbital methods. XXIII A Polarization-type basis set for second-row elements. J Chem Phys 77:3654–3665
54. Hay PJ, Wadt WR (1985) Ab initio effective core potentials for molecular calculations. Potentials for the transition metal atoms Sc to Hg. J Chem Phys 82: 270–283.
55. Hay PJ, Wadt WR (1985) Ab initio effective core potentials for molecular calculations. Potentials for the transition metal atoms Sc to Hg. J Chem Phys 82:284–298
56. Barone V, Cossi M (1998) Quantum calculation of molecular energies and energy gradients in solution by a conductor solvent model. J Phys Chem A 102:1995–2001
57. Cossi M, Barone V (2001) Time-dependent density functional theory for molecules in liquid solutions. J Chem Phys 115:4708–4717
58. O'Boyle NM, Tenderholt AL, Langner KM (2008) Cclib: a library for package-independent computational chemistry algorithms. J Comput Chem 29:839–845
59. Liu X, Zhang N, Zhou J, Chang T, Fang C, Shangguan D (2013) A turn-on fluorescent sensor for zinc and cadmium

ions based on perylene tetracarboxylic diimide. Analyst 138: 901–906
60. Song EJ, Kim H, Hwang IH, Kim KB, Kim AR, Noh I, Kim C (2014) A single fluorescent chemosensor for multiple target ions: recognition of Zn^{2+} in 100 % aqueous solution and F^- in organic solvent. Sensors Actuators B Chem 195:36–43
61. Wang J, Lin W, Li W (2012) Single fluorescent probe displays a distinct response to Zn^{2+} and Cd^{2+}. Chem Eur J 18:13629–13632
62. Kim JH, Noh JY, Hwang IH, Kang J, Kim J, Kim C (2013) An anthracene-based fluorescent chemosensor for Zn^{2+}. Tetrahedron Lett 54:2415–2418
63. Na YJ, Hwang IH, Jo HY, Lee SA, Park GJ, Kim C (2013) Fluorescent chemosensor based-on the combination of julolidine and furan for selective detection of zinc ion. Inorg Chem Commun 35:342–345
64. Job P (1928) Formation and stability of inorganic complexes in solution. Ann Chim 9:113–203
65. Benesi HA, Hildebrand JH (1949) A spectrometric investigation of the interaction of iodine with aromatic hydrocarbons. J Am Chem Soc 71:2703–2707
66. Lin HY, Cheng PY, Wan CF, Wu AT (2012) A turn-on and reversible fluorescence sensor for zinc ion. Analyst 137:4415–4417
67. Lee HG, Kim KB, Park GJ, Na YJ, Jo HY, Lee SA, Kim C (2014) An anthracene-based fluorescent sensor for sequential detection of zinc and copper ions. Inorg Chem Commun 39:61–65
68. Hsieh WH, Wan C, Liao D, Wu A (2012) A turn-on Schiff base fluorescence sensor for zinc ion. Tetrahedron Lett 53:5848–5851
69. Tsui YK, Devaraj S, Yen YP (2012) Azo dyes featuring with nitrobenzoxadiazole (NBD) unit: a new selective chromogenic and fluorogenic sensor for cyanide ion. Sensors Actuators B Chem 161:510–519
70. Garner AL, Koide K (2008) Oxidation state-specific fluorescent method for palladium (II) and platimum (IV) based on the catalyzed aromatic claisen rearrangement. J Am Chem Soc 130:16472–16473
71. Kumar YP, King P, Prasad VSKR (2006) Zinc biosorption on *Tectona grandis* L.f. leaves biomass: equilibrium and kinetic studies. Chem Eng J 124:63–70
72. Lee HG, Lee JH, Jang SP, Park HM, Kim S, Kim Y, Kim C, Harrison RG (2011) Zinc selective chemosensor based on pyridyl-amide fluorescence. Tetrahedron 67:8073–8078
73. Formica M, Fusi V, Giorgi L, Micheloni M (2012) New fluorescent chemosensors for metal ions in solution. Coord Chem Rev 256:170–192